THE JOURNAL OF BIOLOGICAL CHEMISTRY VOL. 284, NO. 2, pp. 954–965, January 9, 2009

Lipid-engineered *Escherichia coli* Membranes Reveal Critical Lipid Headgroup Size for Protein Function*

Received for publication, June 12, 2008, and in revised form, October 23, 2008 Published, JBC Papers in Press, November 3, 2008, DOI 10.1074/jbc.M804482200

Malin Wikström[‡], Amélie A. Kelly[‡], Alexander Georgiev[‡], Hanna M. Eriksson[‡], Maria Rosén Klement[‡], Mikhail Bogdanov[§], William Dowhan[§1], and Åke Wieslander[‡2]

From the [‡]Department of Biochemistry and Biophysics, Stockholm University, Stockholm 10691, Sweden and the [§]Department of Biochemistry and Molecular Biology, University of Texas School of Medicine, Houston, Texas 77225

Escherichia coli **membranes have a substantial bilayer curvature stress due to a large fraction of the nonbilayer-prone lipid phosphatidylethanolamine, and a mutant (AD93) lacking this lipid is severely crippled in several membrane-associated processes. Introduction of four lipid glycosyltransferases from *Acholeplasma laidlawii* and *Arabidopsis thaliana*, synthesizing large amounts of two nonbilayer-prone, and two bilayer-forming gluco- and galacto-lipids, (i) restored the curvature stress with the two nonbilayer lipids, and (ii) diluted the high negative lipid surface charge in all AD93 bilayers. Surprisingly, the bilayer-forming diglucosyl-diacylglycerol was almost as good in improving AD93 membrane processes as the two nonbilayer-prone glucosyl-diacylglycerol and galactosyl-diacylglycerol lipids, strongly suggesting that lipid surface charge dilution by these neutral lipids is very important for *E. coli*. Increased acyl chain length and unsaturation, plus cardiolipin (nonbilayer-prone) content, were probably also beneficial in the modified strains. However, despite a correct transmembrane topology for the transporter LacY in the diglucosyl-diacylglycerol clone, active transport failed in the absence of a nonbilayer-prone glycolipid. The corresponding digalactosyl-diacylglycerol bilayer lipid did not restore AD93 membrane processes, despite analogous acyl chain and cardiolipin contents. Chain ordering, probed by *bis*-pyrene lipids, was substantially lower in the digalactosyl-diacylglycerol strain lipids due to its extended headgroup. Hence, a low surface charge density of anionic lipids is important in *E. coli* membranes, but is inefficient if the headgroup of the diluting lipid is too large. This strongly indicates that a certain magnitude of the curvature stress is crucial for the bilayer *in vivo*.**

Both soluble and membrane proteins may critically interact with or respond to specific lipids, lipid domains, or global bilayer properties (1). Membrane lipids have several general functions. (i) Forming the bulk bilayer with "liquid" chains and insulating properties. The major species tend to be zwitterionic or uncharged and with a smaller fraction of anionic lipids. (ii) Minor lipids constitute signaling molecules and/or identity tags for membrane vesicle traffic. (iii) Lipids are also potential structural/functional cofactors in membrane protein three-dimensional structures (2, 3). (iv) Specific lipids or lipid environments are required during folding of some membrane proteins (4–6).

Maintenance of the liquid state and a certain lipid surface anionic charge density, or surface potential, is important and extensively regulated in most types of cells. Many bacteria, and several eukaryotic organelles also contain a significant level of polar lipid species that due to their smaller headgroup size (and often with no net charge) are prone to form nonbilayer (NB)[3] aggregates. Such lipids increase chain ordering due to a closer lateral packing and increase the tendencies for monolayers to curl concavely, modifying the lateral stress profile ("curvature elastic stress") of each monolayer (7). These collective bilayer properties have been found important for protein function *in vitro*. The curvature bilayer stress seems to be an active and important regulatory mechanism in several bacteria (8, 9), and in the eukaryote *Saccharomyces cerevisiae* (10).

An engineered *Escherichia coli* strain (AD93) lacking its dominant and nonbilayer-prone lipid phosphatidylethanolamine (PE, zwitterionic) (11) is defective or malfunctions in several membrane-associated cellular functions: cell growth and division (12, 13), dependence on divalent cations (14, 15), osmotic stress response and membrane permeability (16), and function/topology of several secondary membrane transporters (4–6). For most of these processes, the exact coupling to membrane bilayer properties is not known. However, introduction by genetic means into AD93 of an enzyme (alMGS) from *Acholeplasma laidlawii* (17) that synthesizes substantial amounts of a "foreign" nonbilayer-prone lipid, glucosyl-diacylglycerol (GlcDAG) restored or improved several of the above cell properties (16). It was suggested that GlcDAG can substitute for PE in at least three ways: (i) provides an increase in NB-prone lipid and curvature stress; (ii) dilutes the high negative lipid charge density; and (iii) provides chemical properties similar to the PE headgroup. Especially the ability of both PE and GlcDAG to

* This work was supported, in whole or in part, by National Institutes of Health Grant R37 GM20478 (to W. D.). This work was also supported by the Swedish Research Council and the Wenner-Gren Foundations (to Å. W.). The costs of publication of this article were defrayed in part by the payment of page charges. This article must therefore be hereby marked "*advertisement*" in accordance with 18 U.S.C. Section 1734 solely to indicate this fact.

[1] To whom correspondence may be addressed. Tel.: 713-500-6051; Fax: 713-500-0652; E-mail: William.Dowhan@uth.tmc.edu.

[2] To whom correspondence may be addressed. Tel.: 46-8-162463; Fax: 46-8-153679; E-mail: ake@dbb.su.se.

[3] The abbreviations used are: NB, nonbilayer; DAG, diacylglycerol; GlcDAG, glucosyl-DAG; GlcGlcDAG, diglucosyl-DAG; GalDAG, galactosyl-DAG; GalGalDAG, digalactosyl-DAG; GT, glycosyltransferase; PE, phosphatidylethanolamine; PG, phosphatidylglycerol; CL, cardiolipin (diphosphatidylglycerol); alMGS and alDGS, GlcDAG and GlcGlcDAG synthases (glucosyltransferases) from *A. laidlawii*; 18:1c, oleic acid; 18:3c, linolenic acid; *bis*-PBPC, 1,2-*bis*-(1-pyrenebutanoyl)-*sn*-glycero-3-phosphocholine; *bis*-PDPC, 1,2-*bis*-(1-pyrenedecanoyl)-*sn*-glycero-3-phosphocholine; MPB, 3-(N-maleimidylpropionyl) biocytin; TM, transmembrane; TMG, methyl-β-D-galactopyranoside; IPTG, isopropyl 1-thio-β-D-galactopyranoside; PC, phosphatidylcholine; WT, wild type.

participate in hydrogen-bond networks was considered important (16). In the GlcDAG strain correct membrane topology for the LacY and uphill transport function were indeed restored (18). The "diluted" negative charge character of the *E. coli* wild type lipid bilayer surface is of primary importance for topogenesis of LacY (19), and the lipid surface must be similarly diluted in the GlcDAG strain compared with the high negative surface charge density in AD93.

In *A. laidlawii* bilayer curvature stress is tightly regulated by a consecutively acting enzyme (alDGS), adding a second glucose moiety to the NB-prone GlcDAG and yielding diglucosyl-DAG (GlcGlcDAG), which is a bilayer-forming lipid due to its substantially larger headgroup (20, 21). Together, these enzymes seem to form a robust feedback mechanism for controlling lipid bilayer global packing properties (22). Analogous features may operate in plant chloroplast thylakoids, dominated by the nonbilayer-prone galatosyl-diacylglycerol (GalDAG), followed by the bilayer-forming digalatosyl-diacylglycerol (GalGalDAG) (23). The corresponding galactosyltransferases, as well as metabolic regulation of these lipids, have similarities to the *A. laidlawii* system (24). However, plant lipids are strongly enriched in polyunsaturated acyl chains, to an extent not tolerated by *A. laidlawii* or *E. coli* (25). Hence, curvature features are analogous but bulk hydrophobic properties, and sugar orientation and inter-sugar bond positions, differ between the chloroplast and *A. laidlawii* glycolipid headgroups. In plants there also seems to be a correlation between curvature stress (*i.e.* balance GalDAG/GalGalDAG), and thermotolerance (26) or (water) drought stress (27).

By introduction of the four glycosyltransferases from *A. laidlawii* and *Arabidopsis thaliana* synthesizing the GlcDAG and GlcGlcDAG, and GalDAG and GalGalDAG pairs, respectively, into the PE-minus (AD93) clone, we intended to address two related questions for the importance of bilayer curvature stress in *E. coli.* (i) Is the improvement brought by the GlcDAG lipid in the PE-minus strain due to its nonbilayer (curvature stress) properties; or (ii) is it caused more by a dilution of the very high anionic lipid surface charge in this strain.

EXPERIMENTAL PROCEDURES

Construction of E. coli Lipid Mutants—E. coli strain AL95 (*pss93*::*kan*^{R} *lacY*::*Tn9*) was used as the host strain is unable to synthesize PE unless it is supplemented with plasmid pDD72 (*pssA*$^+$ *cam*^{R}) (4). Construction of AD93/pTMG3 (GlcDAG strain) and AD93/pDD72 was previously described (16). AD93/pTMG3/pACYCT7DGS (GlcGlcDAG strain) was constructed from AD93/pTMG3 as follows. The *ALdgs* gene was excised from the pET15b-alDGS construct (15) using restriction enzymes NdeI and HindIII and cloned into the vector pACYC-T7 (28). The plasmid was then transferred into AD93/pTMG3 (GlcDAG *E. coli* strain) cells, and plated on LB-plates with 34 μg/ml chloramphenicol, 100 μg/ml ampicillin, 25 μg/ml kanamycin. The coding region of *atMGD1* from *A. thaliana* was amplified without the N-terminal signal peptide by PCR using oligonucleotides PAK 78 (ga cat atg gga gga gtc gga tta tcg ag) and PAK 79 (ct gga tcc aga tta ggc agt gca aga gag). The PCR product was then cloned into the pTMG3 plasmid (16), from which the *ALmgs* fragment had been removed. The entire coding region of *atDGD2* from *A. thaliana* was amplified by PCR using oligonucleotides PAK80 (gg cat atg acg aat cag cag gag caa cac) and PAK 81 (ctg gat ccg tca atc ttg ctt gcg agt att tgg). The PCR product was then cloned into the pACYC-T7-DGS plasmid (this study), from which the alDGS fragment had been removed.

Where indicated these strains also carried the following plasmids: pLacY[13C or 205C], encoding ampicillin resistance and a cysteine-less LacY derivative (dependent on IPTG for expression) in which either G13 or H205 was replaced by cysteine (4); pTMG-LacY[13C or 205C], encoding ampicillin resistance, the GlcDAG synthase (alMGS) (constitutively expressed) and the respective LacY derivative carried in the previous plasmids (18); pACYC-T7-DGS, encoding chloramphenicol resistance, and the GlcGlcDAG synthase alDGS (dependent on IPTG for expression).

Growth Conditions—Bacteria were grown in LB broth containing 5 g/liter NaCl and 10 mM $MgCl_2$ at 30 °C. Plasmids were maintained by supplementing growth media with 50 μg/ml ampicillin (or carbenicillin) and 20 μg/ml chloramphenicol, respectively. IPTG (1 mM) was present in all experiments with expression of GlcGlcDAG, GalGalDAG, or LacY. During growth with $MgCl_2$, the cells were first grown overnight in 2 mM $MgCl_2$ before they were inoculated to the same absorbance in the different media. LacY strains were cultured in LB medium lacking NaCl and containing 10 mM $MgCl_2$. All determinations involving LacY were done on cultures that reached a similar final cell density of $A_{600} = 0.5$.

Acyl Chain Determination—Lipid concentration and acyl chain composition were determined as fatty methyl esters by gas liquid chromatography. Overnight cultures were pelleted in glass tubes and lipid acyl chains esterified by 1 ml of 1 N HCl in methanol. An internal standard of methylated 15:0 was added and samples were incubated at 80 °C for 20 min. After cooling, 1 ml of 0.9% NaCl and 1 ml of hexane were added and samples were shaken vigorously and then centrifuged at 1,000 × *g* for 3 min. Hexane phase was transferred into a fresh glass tube and acyl chain methyl esters were concentrated by a N_2 stream and measured on a gas chromatograph (Hewlett Packard model 5890; DB25 column). Peaks were compared with proper reference mixtures run identically. Acyl chain composition of the various glycolipids was also determined, after isolating the respective lipids by TLC and eluting them by chloroform/methanol (2:1, v/v).

Lipid Analysis—For radiolabeling the lipids, overnight cell cultures were inoculated into LB medium containing 0.2 μCi/ml [^{14}C]acetic acid. After 24 h cells were harvested by centrifugation, and lipids were extracted from cell pellets by extensive stirring in chloroform/methanol (2:1) followed by centrifugation and a second extraction in methanol. The lipids were concentrated by evaporation, separated on Silica Gel 60 TLC plates (Merck) in methyl acetate, isopropyl alcohol, chloroform, methanol, 0.25% KCl (25:25:25:10:9, v/v) or chloroform, methanol, acetic acid (65:25:10, v/v/v), and visualized and quantified by electronic autoradiography (Packard, Fuji, or Bio-Rad imagers). Lipids were identified by mobilities relative to known standard lipids, and by a positive color reaction with orcinol or α-naphtol.

Osmotic Stress Experiments—15-ml sterile falcon tubes were prepared with different concentrations of salts in LB containing 5 g/liter NaCl with 10 mM $MgCl_2$ in a total volume of 5 ml. The same amount of cells (overnight culture) was inoculated in all samples, which were incubated for 24 h at 30 °C at 150 strokes/min in a water bath shaker. Absorbance at 600 nm was measured regularly.

Light Microscopy—*E. coli* cell length distribution was viewed with a Carl Zeiss phase-contrast microscope. Cell lengths were determined by picking random viewing areas and measuring at least 200 cells by an eyepiece with a calibrated grading scale. Membranes were stained by adding 1 μM FM4-64 (Molecular Probes) to overnight cultures and stirred for 3 h at 30 °C before washing three times with phosphate-buffered saline. Potential formation of intracellular membranes by alMGS in AD93/pTMG3 was compared with alMGS expressed from the strong T7 promoter in vector pET15b carried in *E. coli* BL21(DE3) (*cf.* Ref. 16). On the microscope slides the cells were mixed 1:1 (v/v) with 0.7% low-melting agarose. Cells were viewed with a Zeiss Axioplan 2 fluorescence microscope (rhodamine filter). Images were captured with a CCD camera (Sony), and Image Access 3.0 software (Imagic Bildverarbeitung AG).

Membrane Permeability—Permeability of cell membranes was assayed by antibiotic sensitivity, using susceptibility test discs (Oxoid, England). All discs contained 30 μg of the antibiotics except for rifampicin, which was at 50 μg and polymyxin B, which was 35.7 μg. Equal amounts of cells were spread on LB agar plates before the discs were positioned. Plates were incubated for 24 h at 30 °C before measurements of growth inhibition zones.

Pyrene Lipid Probes—Pyrene-labeled lipids 1,2-*bis*-(1-pyrenedecanoyl)-*sn*-glycero-3-phosphocholine (*bis*-PDPC) and 1,2-*bis*-(1-pyrenebutanoyl)-*sn*-glycero-3-phospho-choline (*bis*-PBPC) were from Molecular Probes. The lipid probes (in chloroform) were added to the lipid samples (before liposome preparation) to 0.1% (mol/mol).

Preparation of Liposomes—Lipid mixtures of the desired composition or membrane lipid extracts solubilized in chloroform, methanol (2:1) (v/v) were dried under a stream of nitrogen (gas) and then under reduced pressure for more than 1 h. The dry lipids were hydrated in 500 μl of buffer (0.5 mM lipid concentration) containing 20 mM HEPES and 100 mM sodium maleate, pH 8, by repeated agitation with two glass beads during 45 min. Large unilamellar vesicles (100 nm) were made by 19 successive extrusions of the lipid dispersions through double 100-nm pore size polycarbonate filters (Whatman, UK) with a LiposoFast small volume homogenizer (Avestin, Ottawa, ON), as described (29, 30).

Fluorescence Measurements—The liposome preparations (with probes) were diluted 20 times with 20 mM HEPES, 100 mM sodium maleate, pH 8, to 25 μM final lipid concentration, in a magnetically stirred 1 × 1-cm four-window quartz cuvette. After temperature equilibration at 25 °C, the samples were excitated at 344 nm and emission spectra were collected between 360 and 540 nm on a Fluorolog-3 spectrofluorimeter (Jobin Yvon). Slits of 5 nm were used, and the signal was integrated over 0.2-s intervals. The ratio between the maximum emission by monomeric pyrene (I_m) and by excimer complex formed by an exited pyrene and a ground state pyrene (I_e) was used as a measure of the chain order in the hydrophobic core of the lipid bilayer (31, 32). The ratio I_e/I_m was calculated as I_{480}/I_{394} (*bis*-PDPC) or I_{480}/I_{398} (*bis*-PBPC). Analyses were repeated several times, data from the series prepared and analyzed during the same day are shown.

LacY Topology Determination—The substituted cysteine accessibility method applied to transmembrane (TM) domains (SCAM™), based on the controlled membrane permeability of the thiol-specific reagent 3-(*N*-maleimidylpropionyl) biocytin (MPB), was used to probe the TM topology of LacY as previously described (4, 33). Biotinylation of exposed cysteine residues in whole cells (periplasmic exposure) or only after sonication (cytoplasmic exposure) was detected using a Fluor-S™ MultiImager (Bio-Rad) after SDS-polyacrylamide electrophoresis and Western blotting using avidin linked to horseradish peroxidase to detect biotinylated LacY.

LacY Transport Function—LacY transport function was determined as previously reported (34). Uptake of [^{14}C]TMG (methyl-β-D-galactopyranoside) at a final concentration of 0.1 mM was determined in intact *E. coli* cells as a measure of energy dependent uphill transport function. Uptake of [^{14}C]lactose (final concentration 0.4 mM) was determined in intact *E. coli* cells, which contained β-galactosidase, as a measure of energy independent downhill transport function.

RESULTS

Lipid Engineering of E. coli—By inactivation of the *pssA* gene in *E. coli* otherwise wild type for phospholipid synthesis, the pathway for PE biosynthesis was completely blocked resulting in a mutant now dependent on Mg^{2+} for survival (11), see Fig. 1. By selective introduction of the genes for four lipid glycosyltranferases, clones synthesizing major neutral bacterial and plant glycolipids were obtained. The source of the enzymes and the foreign lipid produced are as follows: *A. laidlawii*, GlcDAG (1,2-diacyl-3-*O*-(α-D-glucopyranosyl)-*sn*-glycerol) and GlcGlcDAG (1,2-diacyl-3-*O*-[α-D-glucopyranosyl-(1→2)-*O*-α-D-glucopyranosyl]-*sn*-glycerol); and *A. thaliana*, GalDAG (1,2-diacyl-3-*O*-(β-D-galactopyranosyl)-*sn*-glycerol) and GalGalDAG (1,2-diacyl-3-*O*-[α-D-galactopyranosyl-(1→6)-*O*-β-D-galactopyranosyl]-*sn*-glycerol), respectively (Fig. 1). These lipids should yield varying curvature stress features due to their nonbilayer-prone and bilayer-forming packing characters (*cf.* Fig. 1). Furthermore, the differences in glucose and galactose headgroup properties (35) will be revealed in the same cell type and with similar lipid acyl chains.

Lipid Composition and Properties in Clones—Wild-type *E. coli* has approximately 75 mol % PE with the remaining fraction being primarily the anionic phospholipids PG (20%) and CL (5%). Strain AD93 (PE-minus) supplemented with the *ALmgs* gene synthesizes substantial amounts of GlcDAG; see Fig. 2*A*. Introduction of the *ALdgs* gene (on a separate plasmid) into the GlcDAG clone yielded GlcGlcDAG as the major lipid. In *A. laidlawii* GlcDAG is the acceptor substrate for GlcGlcDAG synthesis. Induction of the *ALdgs* gene to various extents only marginally affected the GlcGlcDAG amounts, rising from just below 50 mol % without inducer to slightly below 60% at 1 mM IPTG (data not shown). Individual glycolipid

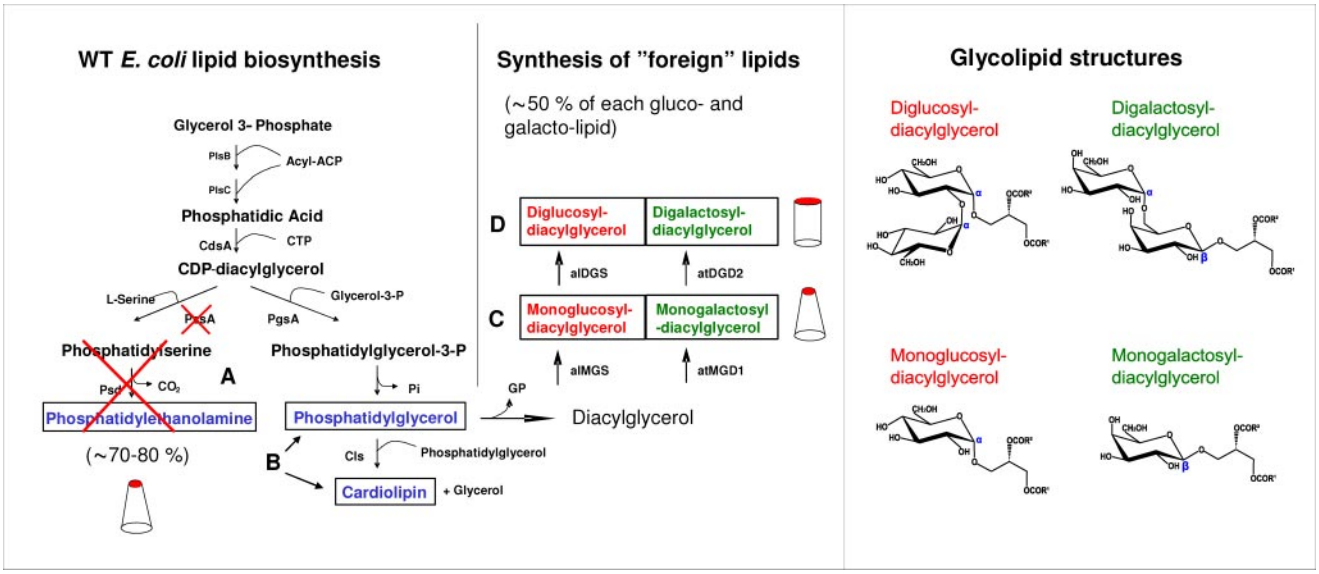

FIGURE 1. **Membrane lipid biosynthesis in *E. coli* lipid mutant strains.** Major wild type lipids are indicated in *blue*, and introduced lipids in *red/green*. *A*, by transposon inactivation (11) of the *pssA* gene, PE production is abolished (indicated by *red crosses*). A wild type phenotype was created by reintroduction of *pssA* on a plasmid. *B*, PG and CL synthesized by the PE-minus AD93 strain (requiring Mg^{2+}). *C*, new monosaccharide-glycolipids synthesized in AD93 complemented with *A. laidlawii* and *A. thaliana* alMGS and atMGD1 glycosyltransferase genes, respectively (both strains PE-minus). *D*, disaccharide-glycolipids synthesized by *A. laidlawii* alDGS and *A. thaliana* atDGD2 glycosyltransferase enzymes, by complementation of the two constructs in *C*. *Cones* and *cylinder schematics* symbolize the packing shapes of the indicated lipids. Structures of the corresponding GlcDAG, GalDAG, GlcGlcDAG, and GalGalDAG glycolipids are indicated to the *far right*. Note the differences in sugar composition, linkage, and orientation.

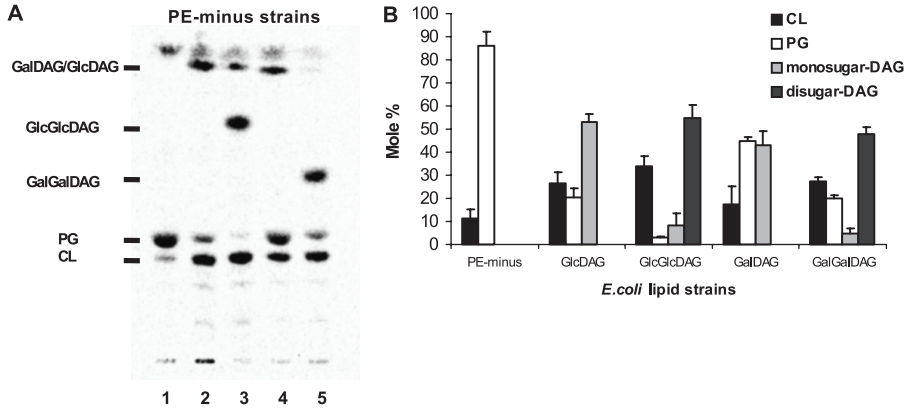

FIGURE 2. **Membrane lipid composition of engineered *E. coli* strains.** Lipids were labeled with [^{14}C]acetic acid during growth for 24 h in LB broth with 5 g/liter NaCl and 10 mM $MgCl_2$, extracted, separated by TLC (methyl acetate system), and quantified as described under "Experimental Procedures." *A*, *lane 1*, strain AD93 (PE-minus); *lane 2*, strain AD93 with plasmid pTMG3 (PE-minus/GlcDAG); *lane 3*, strain AD93 with plasmid pTMG3 and plasmid pACYCT7DGS (PE-minus/GlcDAG/GlcGlcDAG); *lane 4*, strain AD93 with plasmid pTMG3MGD1 (PE-minus/GalDAG); *lane 5*, strain AD93 with plasmid pTMG3 and plasmid pACYCT7DGS (PE-minus/GalDAG/GalGalDAG). *B*, molar percentages of the major lipid species in cells grown to stationary phase. *Error bars* indicate the S.D. for at least three determinations.

amounts above 60 mol % may not be achieved, because this never occurs in the natural *A. laidlawii* host and is rarely observed for other glycolipids in nature. Introduction of the *atMGD1* gene into AD93 yielded slightly lower amounts of GalDAG than for the GlcDAG strain. However, introducing the *atDGD2* gene to this new GalDAG strain produced higher amounts of GalGalDAG lipid with 1 mM IPTG induction (than with 0 mM). The lipid compositions of AD93 (PE-minus), GlcDAG, GlcGlcDAG, GalDAG, and GalGalDAG clones are shown in Fig. 2*B*. The foreign glycolipids all reached close to 50 mol %, or more. Also note the (i) increased cardiolipin content in all modified clones, (ii) strongly decreased PG amounts in the GlcGlcDAG strain, and (iii) decrease of CL in the GalDAG strain, respectively, as compared with the AD93 PE-minus host. The GlcGlcDAG strain also has more glycolipids and less anionic lipids than the GlcDAG strain. Growth without the normal NaCl supplement reduced GlcDAG in the GlcGlcDAG clone close to zero, whereas still maintaining a high GlcGlcDAG fraction, see Fig. 8 below.

Analysis of membrane lipid acyl chain composition (Table 1) revealed that all four glycolipids-containing strains had an increased content of unsaturated chains relative to the AD93 host with (PE-plus), and without (PE-minus), plasmid pDD72, where the GalGalDAG strain was the highest. All except the GlcDAG strain also had increased average acyl chain lengths. Acyl chain features were verified in the purified GlcDAG, GalDAG, GlcGlcDAG, and GalGalDAG lipid species (data not shown). The increased acyl chain unsaturation and length (Table 1) will increase the curvature stress somewhat, potentially to compensate for properties lost, but not fully restored by the foreign lipids. These chain features seem to be the major controllable parameters *in vivo* for *E. coli* lipid-bilayer curvature stress (36), because polar lipid fractions normally are kept fairly constant in the wild type strains. The fraction of CL in the engineered clones may also be important here, because its interaction with divalent cations increases curvature stress and reduces surface anionic charge effects (15, 37).

TABLE 1

Acyl chain composition (in mole %) of the total lipid fraction of lipid strains grown in 1 × LB with 5 g/liter NaCl and 10 mM $MgCl_2$ at 30 °C (*cf.* Figs. 1 and 2)

Acyl chain	PE-plus	PE-minus	GlcDAG	GlcGlcDAG	GalDAG	GalGalDAG
14:0	7.9	6.3	5.2	5.3	4.1	4.4
16:0	40.5	43.8	51.9	37.0	42.2	43.9
16:1c	12.7	15.2	26.2	23.2	16.8	16.3
17:Δ[a]	18.1	8.3	5.3	1.4	1.8	2.6
18:0	1.3	3.8	0.0	5.2	4.2	4.7
18:1c	10.8	14.1	11.4	15.1	22.1	25.4
Unidentified	8.7	8.5	0.0	12.8	8.8	2.7
Unsaturated acyl chains[b]	23.5	29.3	37.6	38.3	38.9	41.7
Saturated acyl chains[b]	67.8	62.2	62.4	48.9	52.3	55.6
Average acyl chain length[b,c]	16.1	16.2	16.1	16.3	16.5	16.5

[a] *cis*-9,10-Methylenehexadecanoic acid.
[b] Unidentified chains are not included.
[c] Average number of backbone carbons in the acyl chains.

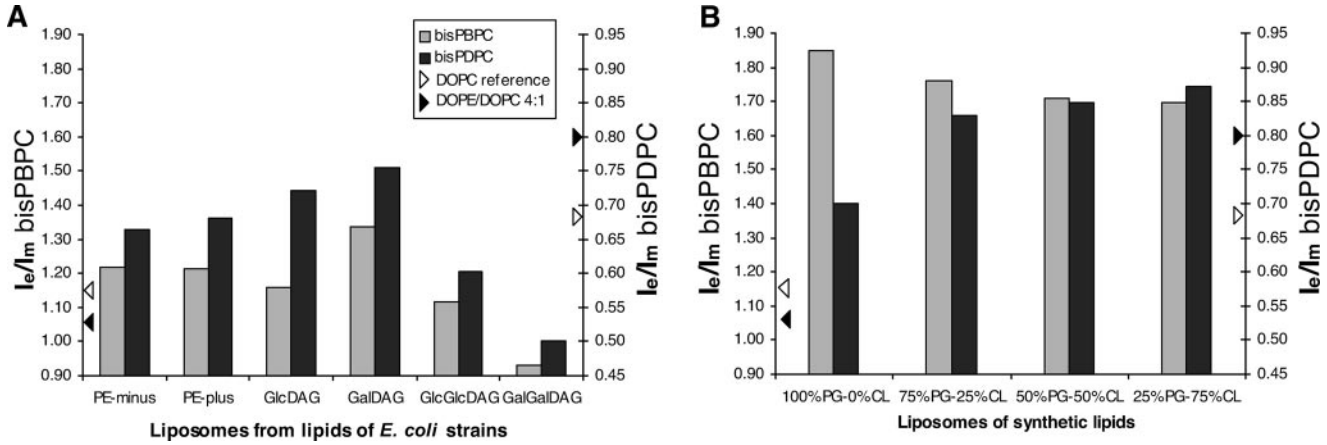

FIGURE 3. **Chain ordering monitored by *bis*-pyrene lipid probes.** The short and long pyrenyl-PC probes *bis*-PBPC (left *y* axes) and *bis*-PDPC (right *y* axes) were used to monitor acyl chain ordering at two bilayer depths, where an increase in I_e/I_m correlates with an increase in chain ordering (40). *A*, polar lipid extracts from the clones as described in the legend to Fig. 2. *B*, mixtures of synthetic dioleoyl-PG and tetraoleoyl-CL. Liposomes were prepared and intramolecular fluorescence parameters I_e and I_m analyzed as described under "Experimental Procedures." *Open/filled triangles* on *y* axes indicate values for established dioleoyl PC/PE reference samples with different curvatures and chain ordering, *cf.* Refs. 39 and 40. Analyses were repeated several times. Each series was prepared and analyzed on the same day.

Chain Ordering by the Foreign Glycolipids—Chain ordering at two different bilayer depths was analyzed by the fluorescent phosphatidylcholine-pyrene probes *bis*-PDPC (higher depth) or *bis*-PBPC (lower depth) in liposomes reconstituted from the *E. coli* clone lipid extracts (Fig. 3*A*). Lipid headgroup size (and charge) affects the lateral area occupied by a single lipid molecule in a bilayer. Smaller headgroups yield closer lipid packing, with increased chain ordering and spontaneous curvature, and consequently changes in the lateral pressure profile along the depth of each monolayer. An increase in the ratio between the maximum emission by the excimer complex formed by an exited pyrene and a ground state pyrene (I_e) and the monomeric pyrene (I_m) correlates with an increase in the chain order in the hydrophobic core of the lipid bilayer (31). Addition of unsaturated PE (NB-prone) to phosphatidylcholine (PC) bilayers substantially increases the spontaneous curvature (39). The concomitant chain order increase is easily monitored by these pyrene probes (40).

Most important, comparing the GlcDAG/GlcGlcDAG and GalDAG/GalGalDAG clones pairwise shows dramatically different chain ordering for the mono- and di-sugar species, slightly larger than between the PC and PE reference samples, despite similar acyl chain compositions within the Glc- and Gal-lipid pairs (Table 1). The PG/CL balance for the clones cannot explain these findings, *cf.* below. The dramatic decrease for the GalGalDAG clone is corroborated by an analogous order decrease caused by stepwise increasing native GalGalDAG (purified from plant) in PC bilayers.[4] Hence, this must mainly be caused by differences in glycolipid headgroup size and orientation, strongly affecting the available lateral space under the headgroups, and hence ordering for the acyl chains.

Liposomes were also made from synthetic di-18:1c-PG and tetra-18:1c-CL mixtures, because PG and CL were major lipids in all the clones (Fig. 2). PG and CL have different head-to-tail volume factors, where CL is more nonbilayer-prone, and both exhibit an increased spontaneous curvature with Mg^{2+} present (41). The charge of free ("unbound") CL in a bilayer is considered to be −1 (and not −2), similar to PG, due to intramolecular H-bonding (reviewed in *e.g.* Ref. 42). The synthetic PG/CL liposomes labeled with the *bis*-PDPC probe showed a clear tendency for increased chain ordering (increasing lateral pressures) at higher depth, with increasing molar contents of CL (Fig. 3*B*). In addition, chain ordering at lower depth (from the shorter *bis*-PBPC probe) slightly decreased with increasing CL content, analogous to increasing PE in the PC/PE mixtures (40).

[4] H. Tjällström and A. Wieslander, unpublished observation.

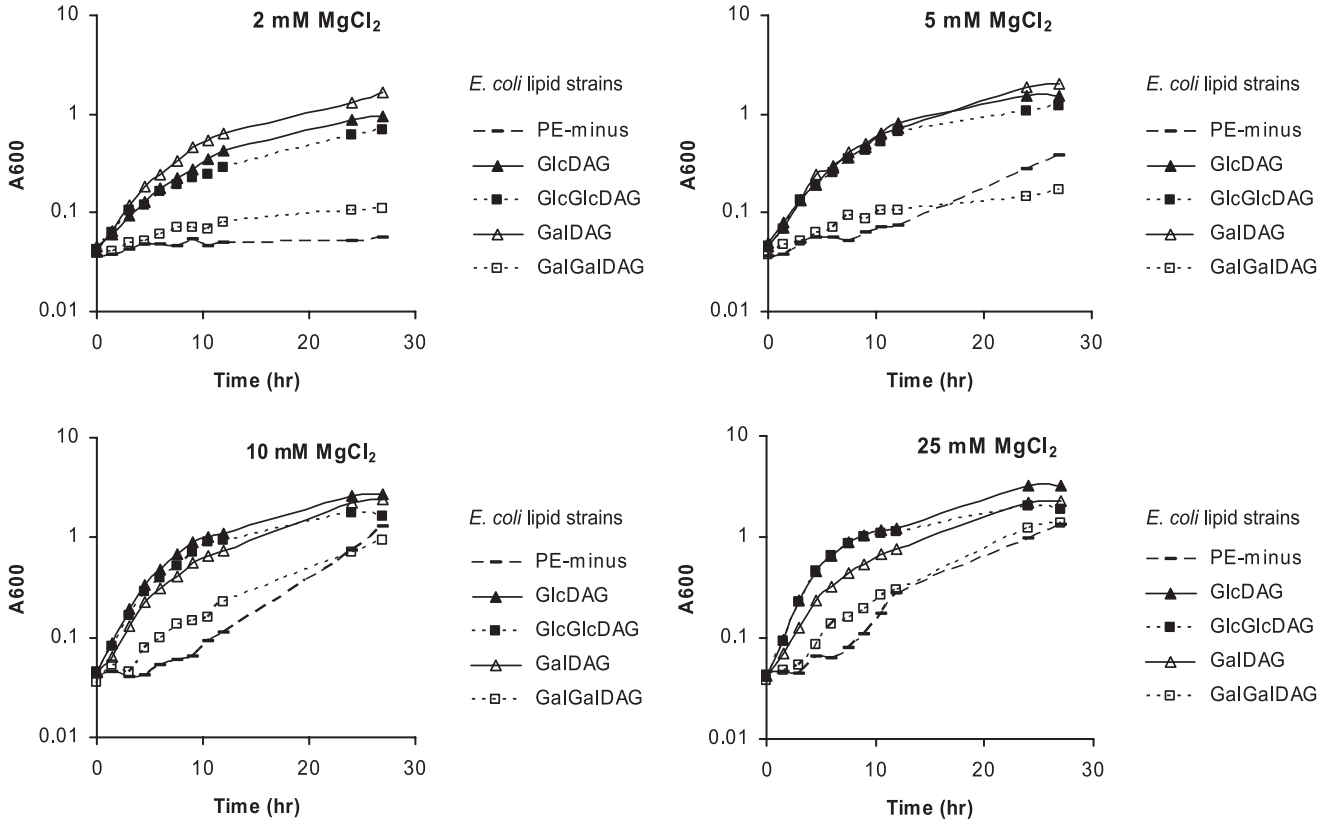

FIGURE 4. **Dependence on Mg^{2+} for glycolipid mutant strains.** Growth curves for AD93 (PE-minus), and AD93 containing the indicated glycolipids grown with different concentrations of $MgCl_2$ are shown; disaccharide-containing strains also contained the respective monosaccharide precursor. Overnight cultures were grown in LB medium (5 g/liter NaCl), and then diluted into LB medium containing $MgCl_2$ at the indicated concentrations, and growth was then followed as a function of A_{600} with a break at 12–22 h (note A_{600} logarithmic scale).

Likewise, the increased magnitude of the I_e/I_m ratios from the longer *bis*-PDPC probe in the PG to CL mixtures (Fig. 3*B*) is similar to that observed for increasing 18:1c-PG in bilayers of 18:1c-GlcGlcDAG or 18:1c-PC, respectively (29). Hence, the PG/CL balance affects chain ordering in lipid bilayers.

In conclusion, the two monosaccharide-glycolipid enriched strains (GlcDAG and GalDAG) revealed an increased chain ordering (especially at larger bilayer depths), which was higher than for the PE-containing (wt) and PE-lacking (PG/CL-enriched) AD93 clone. An extra sugar on each of these glycolipids, yielding the GlcGlcDAG and GalGalDAG species (*cf.* Fig. 1), substantially decreased chain ordering and most dramatically so for the plant GalGalDAG clone (Fig. 3*A*).

Mg^{2+} Dependence and Cell Division—Divalent cations (as Mg^{2+}) are essential for survival and curvature properties of the AD93 mutant. GlcDAG substantially reduced this requirement (16). Growth with different amounts of $MgCl_2$ here showed that the GalGalDAG strain has almost as high a demand for Mg^{2+} as AD93, whereas the other glyco-strains grew much better than AD93 for all tested Mg^{2+} concentrations (Fig. 4). The monosaccharide-DAG strains were the least dependent. At high concentration (25 mM, Fig. 4) the differences between the 5 strains were less than at lower concentrations.

Monitoring cell length as a parameter for cell division, revealed that the GalGalDAG strain has the most perturbed cell division process (Fig. 5). On the other hand, the GlcGlcDAG strain cells were actually shorter than both monosaccharide-DAG strains. AD93 yielded extremely long, multinucleated cells, as recorded before (12). The order of increasing cell lengths for the clones were WT < GlcGlcDAG < GalDAG < GlcDAG < GalGalDAG < AD93 strain, respectively. This length rank does not correlate with chain ordering (Fig. 3), but the lowest (PE-plus), second lowest (GlcGlcDAG), and largest (AD93 strain) total anionic lipid amounts (Fig. 2*B*), yielded the shortest, second shortest, and longest cells, respectively (Fig. 5). However, the varying amounts and curvature stress of CL, and preferential cellular localization (43, 44), may also influence proteins in the cell division process (*e.g.* MinD). Hence, the growth demands for Mg^{2+} seem smaller in clones supplemented with typical NB-prone lipids, and very high in the low-order (*i.e.* low-curvature) GalGalDAG strain, strongly indicating the involvement of this cation in bilayer curvature properties.

Osmotic Stress Tolerance Toward Salts—E. coli has several systems to compensate for intracellular changes upon osmotic up- or down-shifts, *e.g.* compensatory influx or efflux by membrane transporters and gated channels, and synthesis of certain osmolytes. AD93 cells cannot grow at external concentrations of salt higher than about 0.5 M, most likely due to malfunctioning osmo-adaption systems. Fig. 6 reveals the relative growth responses of wild type and glycolipid strains to increasing extracellular KCl and NaCl. K^+ is maintained at high intracellular concentration, whereas Na^+ is actively extruded. However, at high extracellular concen-

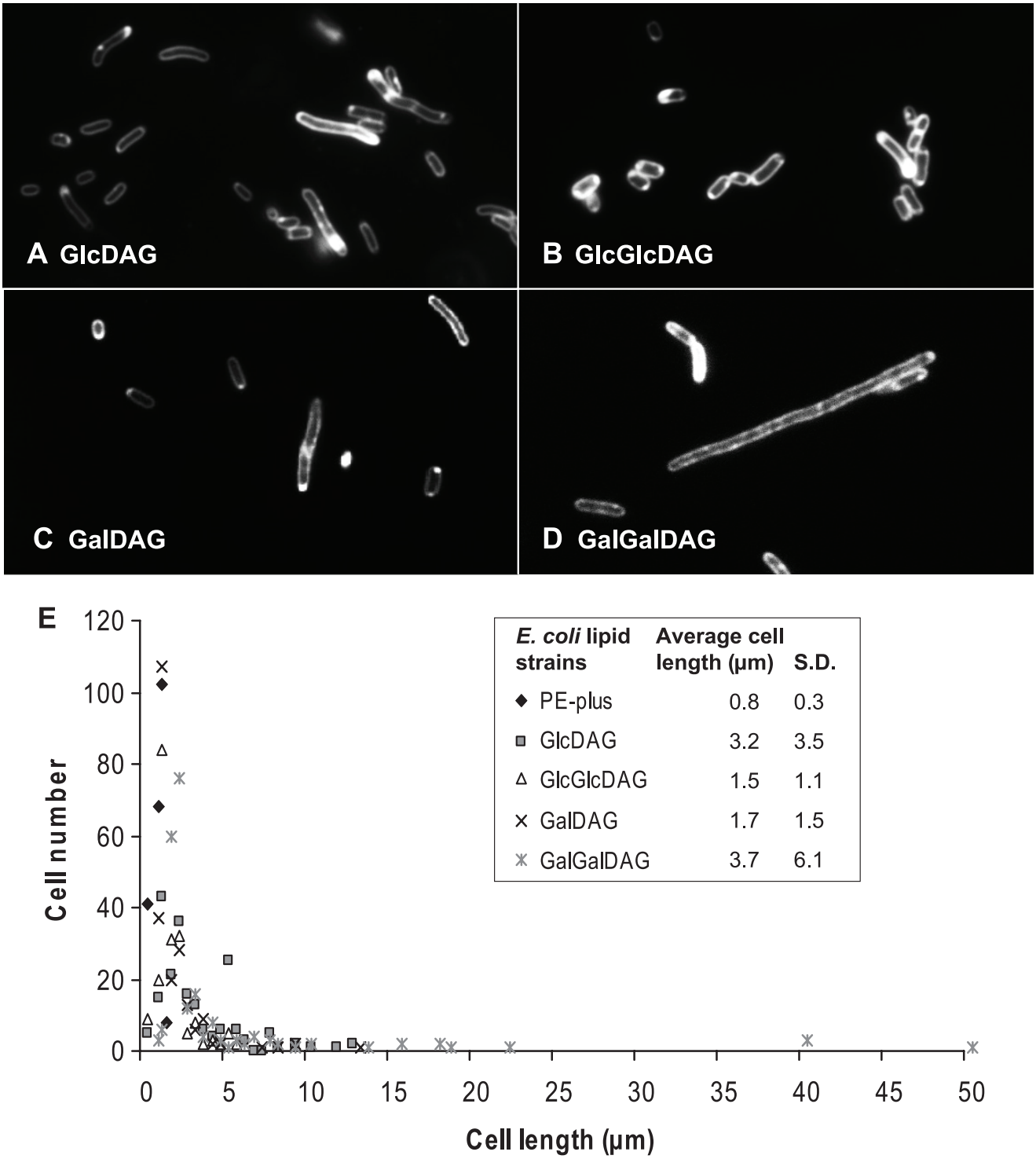

FIGURE 5. **Cell length and morphology of lipid variants.** *A–D*, indicated strains were grown in LB with 10 mM $MgCl_2$ and stained with FM4-64 and viewed with a Zeiss fluorescence microscope (rhodamine filter). Images were captured at ×63 enlargement (ocular −1.25) with a CCD camera. *B*, analysis of cell length for the lipid variants grown in LB medium with 10 mM $MgCl_2$. For the cell length distribution, unstained cells embedded in soft-agar were viewed with a Zeiss light microscope. Cell lengths were determined by picking random areas and measuring at least 200 cells by an eyepiece with a grading scale. Due to the random orientation of the cells in the agar, cell end-views (more common for short cells) are also included. *E*, typical length distributions from *panels A–D*. Short cells position close to zero at this scale (cf. above). AD93 (PE-minus) is ~7 μm. For the GalGalDAG strain the standard deviation illustrates the substantially larger span in cell length.

trations the latter ion "leaks" in at too high a rate for the outward transporters. With both NaCl and KCl the wild type (PE-containing) and GlcGlcDAG strains showed very similar behavior (Fig. 6). The GlcDAG strain was even stimulated at low-to-medium NaCl concentrations, indicating that the intracellular concentrations are lower here than in the WT, and need osmotic compensation by increased extracellular concentrations. Hence, with respect to growth during osmo-

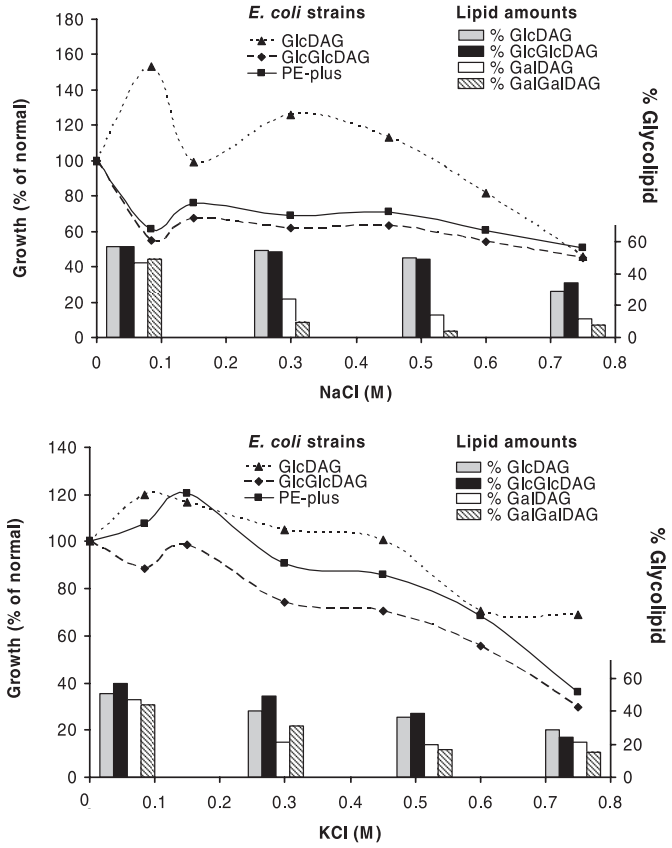

FIGURE 6. **Osmotic stress tolerance.** Growth (A_{600}) was compared after 24 h at 30 °C in supplemented LB medium, relative to conditions without added osmolytes (% of normal growth). *Line graphs*, effects of different NaCl (*A*) and KCl (*B*) total concentrations on cell growth are shown by the three curves (*left x* axis). *Bar graphs*, mole % (*right x* axis) of the indicated glycoplipids in each strain, respectively, and at different salt concentrations, as revealed by radiolabeling.

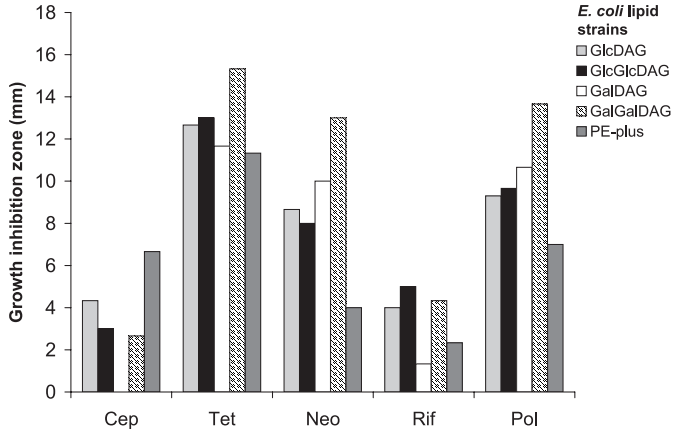

FIGURE 7. **Membrane permeability of *E. coli* glycolipid strains.** Agar plates with antibiotic discs were grown for 24 h before measurement of the inhibitory growth zone around the discs. Almost identical data (maximum difference 1 mm) were obtained from three series of experiments and the averages are shown. Note that the GalDAG clone is resistant to Cep and therefore not shown. Strain AD93/pDD72 is indicated by *PE-plus*.

adaption the GlcGlcDAG strain performs as the WT, and slightly different to the GlcDAG strain.

Both the alMGS and alDGS enzymes are dependent on anionic lipid headgroups, and activity can be reduced by quenching lipid charge by increasing salt *in vitro*. Hence, glucolipid amounts went down with increased salt concentration, as shown in Fig. 6. Surprisingly low amounts of the bilayer-prone GlcGlcDAG lipid at the highest salt concentrations could still support growth (Fig. 6), which was zero in the AD93 (PE-minus) host (data not shown). Here, the compensatory increase in PG amounts was larger than for CL when GlcGlcDAG went down (data not shown). The growth properties for the galactolipid mutants could not be compared in these experiments, because the galactolipid amounts dropped drastically even at moderate external salt concentrations (Fig. 6), and they behaved essentially as the non-growing AD93 host especially under the high salt stress conditions (data not shown). This indicates differences in membrane binding of the *A. laidlawii* and the *Arabidopsis* enzymes.

Glycolipids Increase Cell Permeability—Antibiotics have to cross the outer membrane and sometimes the inner membrane of *E. coli* by passive diffusion to reach their different cellular targets. In the outer membrane the porins allow passage for sufficiently small molecules. By using antibiotics with various intracellular targets, the "permeability" of these two membranes can be assessed by analyzing colony growth inhibition zones (16) (Fig. 7). Cephalothin and vancomycin have to cross the outer membrane to reach the cell wall synthesis target. Neomycin and rifampicin cross both membranes to block protein synthesis, and polymyxin incorporates into the two membranes. The glycolipid strains were more sensitive than the PE-containing strain to all antibiotics except Cep, with the exception of the GalDAG strain being more resistant to Rif. The GalGalDAG strain was more sensitive than the other glycolipid strains for three of the antibiotics. Hence, PE is important for inhibiting passive membrane permeability, and it cannot be replaced with glycolipids. Furthermore, the bilayer of the GalGalDAG strain was somewhat more leaky than the GlcDAG, GalDAG, and GlcGlcDAG strains. Generally, molecules and conditions that lower lipid chain ordering in bilayers, like chain unsaturation and headgroup size, tend to increase the passive transmembrane diffusion. The low chain ordering for the GalGalDAG clone (Fig. 3*A*) may thus be the molecular basis for its increased antibiotic sensitivity, allowing for an increased permeability.

Effect of Lipid Composition on LacY Topology and Transport Function—The differences in lipid composition between the lipid clones results in differences in bilayer surface charge and curvature stress. The *E. coli* secondary membrane transporter LacY requires the presence of PE *in vivo* for uphill (proton-driven) transport of substrate against a concentration gradient, whereas in the AD93 (PE-minus) mutant, only downhill transport is observed (34). In the absence of PE, the N-terminal six-TM helical bundle adopts an inverted transmembrane topology, whereas the remaining ones in the C-terminal bundle are correctly oriented (19). Also *in vitro*, an abnormally high concentration of anionic lipids results in inverted LacY topology (45). Diluting anionic lipids in the AD93 (PE-minus) mutant by synthesis of GlcDAG, also yielding an increased curvature stress, restored correct topology and energy-dependent uphill transport by LacY (16, 18).

Can the bilayer-prone GlcGlcDAG similarly substitute for PE in supporting LacY topology and function *in vivo*, because it

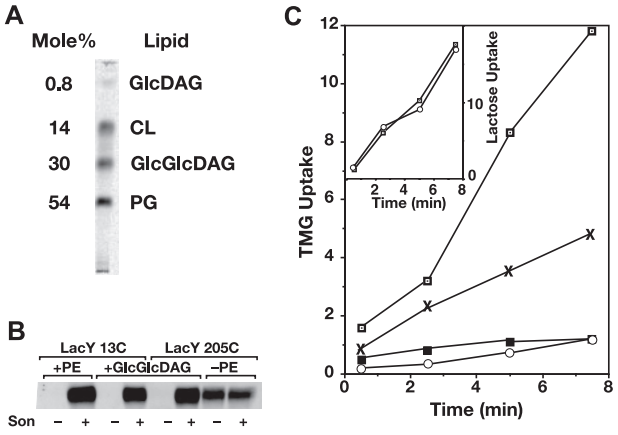

FIGURE 8. **LacY topology and transport activity as a function of lipid composition.** *A*, strain AL95 carrying plasmids pTMG-LacY[13C] and pACYC-T7-DGS was grown (without NaCl at 30 °C) in the presence of [^{14}C]acetate, antibiotics, and IPTG and the lipids analyzed as described under "Experimental Procedures." *B*, strains AL95/pDD72/pLacY[13C] (+PE), AL95/pLacY[205C] (−PE), or AL95/pTMG-LacY[13C or 205C]/pACYC-T7-DGS (+GlcGlcDAG) were grown and analyzed for topological organization of LacY by SCAM™ either before (−) or after (+) sonication (Son) of cells as described under "Experimental Procedures." *C*, strains AL95/pDD72/pLacY[13C] (+PE, *open squares*), AL95/pLacY[205C] (−PE, *closed squares*), AL95/pTMG-LacY[13C] (+GlcDAG, noted by *X*), or AL95/pTMG-LacY[13C]/pACYC–T7–DGS (+GlcGlcDAG, *open circles*) were grown and assayed for uphill transport of TMG (*large panel*) or downhill transport of lactose (*inset*). Uptake of substrate was normalized to nanomole per mg of cell protein. Note the minor fraction of GlcDAG lipid in *A*.

effectively dilutes the anionic lipids in AD93 (Fig. 2*B*)? As shown in Fig. 8*A*, growth of clone GlcGlcDAG-pLacY at 30 °C, with no NaCl and both glucolipid synthases expressed, results in GlcGlcDAG levels of near 30% with only trace levels of GlcDAG and the remaining lipids being primarily PG and CL. Under these conditions LacY appears to be inserted and organized in its wild type topology as it is in WT cells (Fig. 8*B*). Amino acid positions 13 and 205 are in the N-terminal domain and the domain between transmembrane segments VI and VII of LacY, respectively, both of which are fully exposed to the cytoplasmic in wild type cells. These domains are only exposed to MPB labeling after cells are sonicated to disrupt the membrane barrier. Due to the inversion of the N-terminal bundle of LacY in AD93, these residues will now be exposed to the periplasm and biotinylated by MPB without sonication. As shown in the control experiments, LacY-[13C] is only biotinylated after sonication in PE-containing cells, whereas LacY-[205C] is biotinylated without sonication in PE-lacking cells (Fig. 8*B*). In cells lacking PE, but containing GlcGlcDAG, both positions are protected from biotinylation in whole cells but are biotinylated after sonication (Fig. 8*B*), consistent with a native topology for LacY in GlcGlcDAG cells.

However, wild type function appears not to be supported by GlcGlcDAG in the absence of PE (Fig. 8*C*). High levels of uptake of the non-hydrolyzable LacY substrate analogue TMG are coupled to downhill movement of protons and dependent on maintenance of a membrane potential, which is normal in PE-minus cells (34) and reflected in the robust growth of the GlcGlcDAG clone. The low level of TMG uptake observed in PE-lacking cells with and without GlcGlcDAG (Fig. 8*C*) is a result of equilibration of substrate across the membrane, and is not affected by addition of a protonophore that dissipates the proton electrochemical gradient (data not shown). As previously shown (14), when GlcGlcDAG was used to replace PE, significant uptake of TMG was again observed, which rules out any affect of growing cells in the absence of NaCl. Uptake of lactose (Fig. 8*C*, *inset*), which is immediately hydrolyzed by endogenous β-galactosidase, is a measure of energy-independent equilibration of substrate across the membrane (downhill transport), which is supported by GlcGlcDAG as it is in PE-minus cells.

Hence, GlcGlcDAG allows for a correct assembly of LacY in the absence of NB-prone lipids, most likely because the high anionic lipid surface charge is brought down substantially by GlcGlcDAG synthesis, analogous to the case for the GlcDAG. Furthermore, correct topology and downhill transport *in vivo* can obviously be supported at different curvature stress conditions, because the latter are different for these clones. However, LacY seems to demand a critical curvature stress *in vivo* for a functional uphill transport capacity.

DISCUSSION

Type of Lipid Headgroup Is Important—The introduction of genes for foreign lipid glycosyltransferases in a PE-minus *E. coli* strain yielded large amounts of new NB-prone and bilayer-forming membrane lipids (Figs. 1 and 2). The GlcGlcDAG (bilayer-forming) containing *E. coli* performed equally well, or even better than the GlcDAG and GalDAG (NB-prone) strains in several aspects, but failed in others. Yet, whereas GalDAG and GlcDAG are rather similar in their performance, *E. coli* cells accumulating similar amounts of GalGalDAG (bilayer-forming) as the GlcGlcDAG strain (Fig. 2) hardly survive, showing no better performance than the deficient "parent strain" AD93.

The general conclusions are that: (i) cell division proceeded more orderly, with shorter more wild type-like cells for the GlcGlcDAG strain (Fig. 5); (ii) the dependence of the GlcGlcDAG strain on Mg^{2+} ions was close to the GlcDAG strain and much better than for AD93 parent (Fig. 3); (iii) osmo-stress tolerance in the GlcGlcDAG strain was slightly lower than for the GlcDAG strain but fairly similar to the WT; (iv) the permeability toward various antibiotics seemed to be lower for the GlcGlcDAG, GlcDAG, and GalDAG strains than for the GalGalDAG strain, but definitely higher for all four than the WT; (v) proper topology of LacY transporter depends on a dilution of high negative surface charge density, as previously shown (19), rather than curvature bilayer stress; and (vi) uphill transport of lactose by LacY *in vivo* seems to demand, in addition to a correct transmembrane topology, a curvature bilayer stress of a critical magnitude. Hence, a tentative explanation for these observed phenotypes strongly suggests a dilution of the high anionic lipid surface charge in AD93 being the reason for the better general performance of both monosaccharide-DAG strains as well as the GlcGlcDAG strain. However, a certain curvature stress seems important for certain membrane transporters, and these conditions are absent (or lower) in the GlcGlcDAG and GalGalDAG strains. The latter clone is rather comparable with the PE-lacking AD93 parent, which is highly defective in all of these functions.

Lipid Packing Properties and Curvature Stress—Explanations for the observed effects must reside in the properties of the

lipids, and the demands of the various processes on the lipid environment. PE reorganizes into a NB phase at somewhat higher temperatures than GlcDAGs or GalDAGs (35, 46), implying a somewhat lower curvature stress. However, PE amounts in Gram-negative bacteria are commonly larger (75 mol %) than GlcDAG (or GalDAG) amounts (maximum ≈55 mol %). Disaccharide-DAGs are always bilayer-forming, and yield less curvature stress (47), like PG (*cf.* Ref. 48). CL from *E. coli* can form NB phases with divalent cations like Mg^{2+} (37), and curvature may be the reason for survival of the CL-rich (PE-minus) AD93, which requires Mg^{2+} (15). CL amounts in AD93 seem to vary inversely with cation NB-inducing potential and concentration (15), and cells devoid of both PE and CL are not viable. Here, CL amounts rose to over 40 mol % with decreasing GlcGlcDAG at the highest NaCl stress concentrations. Both of the disaccharide-DAG strains have higher amounts of CL than the monosaccharide-DAG strains. This indicates a potential regulation of curvature in *E. coli* by increased CL for the strains lacking NB-prone lipids, as was previously indicated for AD93. Hence, curvature should increase by an increasing membrane fraction of CL.

The importance of Mg^{2+} for curvature was evident here, where the two NB-lipid clones required less ion than the bilayer-lipid strains (Fig. 4). Note that Mg^{2+} increased curvature for both PG and CL. Because the internal concentration is very high (50–100 mM), this may indicate that it is the external Mg^{2+} concentrations that are important, *i.e.* for the outer leaflet of the inner membrane, inner leaflet of the outer membrane, or lipopolysaccharide/outer membrane structural integrity, respectively. Ca^{2+}, which is excluded from the cytoplasm, also supports growth of AD93 (15). The increase of acyl chain unsaturation for all glycolipid strains, and especially for the GalGalDAG strain, might also be a compensatory mechanism for the loss of NB lipids (36). The slight increase of average acyl chain length in the PE-minus, GlcGlcDAG, GalDAG, and GalGalDAG strains, even if small, contributes by also increasing curvature (36). The increase in chain length (Table 1) is of the same magnitude as used by *E. coli* WT to compensate for curvature changes upon a reduction of growth temperature by 20 °C (36).

An additional property of importance is the ability of the polar headgroups to participate in hydrogen bonding. This is common for PE, but PG seems to be the preferred partner (49). However, hydrogen bonding is more extensive for the glycolipids, as indicated from their slower lateral diffusion rates (9). Especially GlcDAG seems not to mix homogenously with the other *A. laidlawii* lipids (including PG) in bilayers but becomes enriched laterally (30). Hence, a replacement of native PE will change interactions for PG, and the foreign glycolipids will maintain some hydrogen-bonding features in the interface regions but introduce different local interactions, which may affect protein organization.

Chain Ordering and Headgroup Configuration—The *bis*-pyrene lipid probes "sense" the chain ordering at different depths in the bilayer, with *bis*-PBPC at chain carbons 5–10 and *bis*-PDPC at carbons 11–16 (40). The somewhat higher ordering (increased I_e/I_m) for the synthetic oleoyl (18:1c) lipids (Fig. 3*B*) is logical given the longer chains here compared with the *E. coli* lipids (Fig. 3*A*). The high ordering for the GalDAG strain (Fig. 3*A*) is probably caused by an upright position of the single β-Gal headgroup, as indicated from NMR analyses (50). The somewhat lower chain ordering in the GlcDAG strain lipids (Fig. 3*A*) should depend on an orientation of the α-Glc headgroup parallel to the interface, as shown by NMR (51), and α-sugar-DAGs have indeed higher transition temperatures for NB formation ("less curvature") than β-sugar-DAGs (35). Both monosaccharide-DAGs have substantially smaller lateral areas in monolayer analyses than their larger disugar-DAG relatives, *e.g.* (52). The $\alpha 1' \rightarrow 6'$ connecting bond for the outer Gal in GalGalDAG is a much more flexible link than the $\alpha 1' \rightarrow 2'$ for the outer Glc in the *A. laidlawii* GlcGlcDAG. In models a very compact conformation for the *A. laidlawii* GlcGlcDAG head, and an extended conformation for the plant GalGalDAG headgroup is evident (53), and supported by NMR analyses (50). Likewise, NMR analyses showed that the acyl chain order in *A. laidlawii* membranes or lipids was substantially lower with high GlcGlcDAG amounts, and higher with low GlcGlcDAG amounts (54).

These headgoup size features must be responsible for the substantially lower chain ordering in the *E. coli* GalGalDAG clone, both at the lower and upper parts of the acyl chains (Fig. 3*A*). The larger lateral area should lower curvature stress possibly below some threshold level achieved in the other strains by CL, Mg^{2+}, chain unsaturation, and length. Hence, for this construct, curvature stress is most likely the critical parameter for cell growth and survival.

Lipid Properties and LacY Function—Various properties of lipids influence the activity of membrane proteins. Optimum translocation activity of the SecYEG translocon complex from *E. coli* or *Bacillus subtilis* was obtained only with the specific lipid composition of each organism (55). Similarly, *E. coli* and chloroplast SecA ATPases are optimally active in their native lipid environment (56). The *E. coli* SecA activity exhibited a clear optimum at 60 mol % of PE and 40 mol % of dioleoyl-PG within a fairly narrow range of PG content. However, chloroplast SecA activity was optimal in GalGalDAG and dioleoyl-PG at a molar ratio of neutral and anionic lipids found in the thylakoid membranes, demonstrating an evolutionary adaptation of protein function to a given lipid composition. The osmotic activation of transporter ProP in *E. coli* is correlated with the molar fraction of CL in the membrane (57). The structure and crystal forms of LacY exhibited a critical dependence on the native lipid to protein ratio employed (58). The topological organization of LacY (19, 34), phenylalanine permease (5), and γ-aminobutyrate permease (6) is dependent on the balance between anionic (PG plus CL) and neutral (PE) lipid. Reduction of the latter below a critical level results in inverted topologies for these proteins.

By comparing the interchangeability and specificity of PE (34), phosphatidylcholine (45), GlcDAG (16, 18), and GlcGlcDAG (this study), the lipid requirement for proper topogenesis of LacY has been assessed. These lipids support the native topology of LacY, the common property is their lack of net charge and therefore the ability to dilute the high negative membrane surface charge contributed by PG and CL. On the other hand as further demonstrated here, PE and GlcDAG, but

not GlcGlcDAG, support uphill transport by LacY suggesting that function requires a neutral NB-prone lipid. The Ca^{2+}-ATPase of the sarcoplasmic reticulum reconstituted with either PE or GalDAG exhibited a high initial rate of ATP-dependent coupled Ca^{2+} uptake (59), but lipids with increasing degrees of methylation (PE, monomethyl-PE, dimethyl-PE, or PC), or increasing degrees of glycosylation (GalDAG *versus* GalGalDAG), revealed a progressive decrease in coupled uptake. Thylakoid lumen violaxanthin de-epoxidase was active when GalDAG or PE was present in the assay mixture but no conversion occurred when only PC or GalGalDAG was present (60). Thus, progressive loss of function, correlated with a shift from NB to bilayer potential for the lipids, appears to be quite general. Only PE and GlcDAG (or GalDAG) share the ability to simultaneously increase curvature stress, form hydrogen bonds, and have no net charge, which differentiates them from CL. Therefore, for optimal membrane protein function these properties should reside within the same lipid molecule.

The importance of a critical curvature stress for active (uphill) transport can be coupled to several molecular mechanisms, like (i) the interface penetration of some (soluble) loops in integral proteins, important for transport; (ii) binding sites or pockets in the proteins, into which only some NB-prone lipids uniquely "fit." Conserved sites for lipid and (sugar) detergent binding are present, *e.g.* cytochrome *c* oxidase (61). (iii) Conformational changes during the transport process, important for H^+ and/or substrate transfer, which may be promoted or prevented by a certain curvature stress. For a photosynthetic reaction center, different curvature stress seems to affect the organization of the entire transmembrane-spanning region, as seen from crystals in two types of lipid/amphiphile environment (62). Therefore, it is evident that NB-prone lipids, or a certain curvature stress, are important for function of a number of proteins. However, support of function is more complex and protein-specific, than effects on topology, which appears to depend on net charge balance (19). Most interesting is an apparent universal interchangeability between PE and glycolipids in support of native topological organization and function.

Evolutionary Aspects—The question why oxygenic photosynthetic organisms contain galactolipids, and not glucolipids, is still an enigma. Cyanobacteria even first synthesize a β-GlcDAG, which is then epimerized to the GalDAG. It was possible to restore overall growth, but not the total photosynthetic capacity of an *A. thaliana* mutant lacking most of its normal αGalβGalDAG by replacing it with βGlcβGalDAG (38). However, the observed differences appeared less dramatic than in this study.

Conclusions—It can be concluded that a low bilayer surface charge density of anionic lipids, and a critical curvature stress, are beneficial for *E. coli* membrane-associated processes. The larger lateral headgroup area occupied by the plant GalGalDAG species brings the membrane toward a much less nonbilayer-prone (less curvature) state, which is out of the "regulation limit" for *E. coli*. This change of lateral pressure in the membrane causes decreased activities of several membrane functions. In contrast, smaller headgroups of lipids (higher curvature) seems to bring advantages for a number of membrane-associated proteins in *E. coli*, as illustrated for LacY active transport.

Acknowledgment—We thank Prof. Lars Wieslander, Stockholm University, for microscope access.

REFERENCES

1. Ces, O., and Mulet, X. (2006) *Signal Transduction* **6,** 112–132
2. Lee, A. G. (2003) *Biochim. Biophys. Acta* **1612,** 1–40
3. Palsdottir, H., and Hunte, C. (2004) *Biochim. Biophys. Acta* **1666,** 2–18
4. Bogdanov, M., Heacock, P. N., and Dowhan, W. (2002) *EMBO J.* **21,** 2107–2116
5. Zhang, W., Bogdanov, M., Pi, J., Pittard, A. J., and Dowhan, W. (2003) *J. Biol. Chem.* **278,** 50128–50135
6. Zhang, W., Campbell, H. A., King, S. C., and Dowhan, W. (2005) *J. Biol. Chem.* **280,** 26032–26038
7. Zimmerberg, J., and Kozlov, M. M. (2006) *Nat. Rev. Mol. Cell Biol.* **7,** 9–19
8. Lindblom, G., Brentel, I., Sjolund, M., Wikander, G., and Wieslander, A. (1986) *Biochemistry* **25,** 7502–7510
9. Lindblom, G., Oradd, G., Rilfors, L., and Morein, S. (2002) *Biochemistry* **41,** 11512–11515
10. Boumann, H., Gubbens, J., Koorengevel, M., Oh, C., Martin, C., Heck, A., Patton-Vogt, J., Henry, S., de Kruijff, B., and de Kroon, A. (2006) *Mol. Biol. Cell* **17,** 1006–1017
11. DeChavigny, A., Heacock, P. N., and Dowhan, W. (1991) *J. Biol. Chem.* **266,** 5323–5332
12. Mileykovskaya, E., Sun, Q., Margolin, W., and Dowhan, W. (1998) *J. Bacteriol.* **180,** 4252–4257
13. Mileykovskaya, E., Fishov, I., Fu, X., Corbin, B. D., Margolin, W., and Dowhan, W. (2003) *J. Biol. Chem.* **278,** 22193–22198
14. DeChavigny, A., Heacock, P. N., and Dowhan, W. (1991) *J. Biol. Chem.* **266,** 10710
15. Rietveld, A. G., Killian, J. A., Dowhan, W., and de Kruijff, B. (1993) *J. Biol. Chem.* **268,** 12427–12433
16. Wikstrom, M., Xie, J., Bogdanov, M., Mileykovskaya, E., Heacock, P., Wieslander, A., and Dowhan, W. (2004) *J. Biol. Chem.* **279,** 10484–10493
17. Berg, S., Edman, M., Li, L., Wikstrom, M., and Wieslander, A. (2001) *J. Biol. Chem.* **276,** 22056–22063
18. Xie, J., Bogdanov, M., Heacock, P., and Dowhan, W. (2006) *J. Biol. Chem.* **281,** 19172–19178
19. Bogdanov, M., Xie, J., Heacock, P., and Dowhan, W. (2008) *J. Cell Biol.* **182,** 925–935
20. Vikstrom, S., Li, L., Karlsson, O. P., and Wieslander, A. (1999) *Biochemistry* **38,** 5511–5520
21. Edman, M., Berg, S., Storm, P., Wikstrom, M., Vikstrom, S., Ohman, A., and Wieslander, A. (2003) *J. Biol. Chem.* **278,** 8420–8428
22. Alley, S. H., Ces, O., Templer, R. H., and Barahona, M. (2008) *Biophys. J.* **94,** 2938–2954
23. Rivas, E., and Luzzati, V. (1969) *J. Mol. Biol.* **41,** 261–275
24. Kelly, A., Sedoud, A., Storm, P., Öhman, A., and Wieslander, Å. (2007) *Proceedings of the 17th Conference of Plant Lipids*, pp. 25–31, Aardvark Global Publ. Co. Salt Lake City, UT
25. Wieslander, A., and Selstam, E. (1987) *Biochim. Biophys. Acta* **901,** 250–254
26. Chen, J., Burke, J. J., Xin, Z., Xu, C., and Velten, J. (2006) *Plant. Cell Environ.* **29,** 1437–1448
27. Torres-Franklin, M. L., Gigon, A., de Melo, D. F., Zuily-Fodil, Y., and Pham-Thi, A. T. (2007) *Physiol. Plant.* **131,** 201–210
28. Nakano, Y., Yoshida, Y., Yamashita, Y., and Koga, T. (1995) *Gene* (*Amst.*) **162,** 157–158
29. Karlsson, O. P., Rytomaa, M., Dahlqvist, A., Kinnunen, P. K., and Wieslander, A. (1996) *Biochemistry* **35,** 10094–10102
30. Storm, P., Li, L., Kinnunen, P., and Wieslander, A. (2003) *Eur. J. Biochem.* **270,** 1699–1709
31. Sunamoto, J., Iwamoto, K., Kondo, H., and Shinkai, S. (1980) *J. Biochem.* (*Tokyo*) **88,** 1219–1226

32. Xiang, T. X. (1993) *Biophys. J.* **65,** 1108–1120
33. Bogdanov, M., Zhang, W., Xie, J., and Dowhan, W. (2005) *Methods* (*San Diego*) **36,** 148–171
34. Bogdanov, M., and Dowhan, W. (1995) *J. Biol. Chem.* **270,** 732–739
35. Mannock, D. A., and McElhaney, R. N. (2004) *Curr. Opin. Colloid Interface Sci.* **8,** 426–447
36. Morein, S., Andersson, A., Rilfors, L., and Lindblom, G. (1996) *J. Biol. Chem.* **271,** 6801–6809
37. Killian, J. A., Koorengevel, M. C., Bouwstra, J. A., Gooris, G., Dowhan, W., and de Kruijff, B. (1994) *Biochim. Biophys. Acta* **1189,** 225–232
38. Holzl, G., Witt, S., Kelly, A. A., Zahringer, U., Warnecke, D., Dormann, P., and Heinz, E. (2006) *Proc. Natl. Acad. Sci. U. S. A.* **103,** 7512–7517
39. Marsh, D. (2007) *Biophys. J.* **93,** 3884–3899
40. Templer, R. H., Castle, S. J., Curran, A. R., Rumbles, G., and Klug, D. R. (1998) *Faraday Discuss.* **111,** 41–53; Discussion 69–78
41. Alley, S. H., Ces, O., Barahona, M., and Templer, R. H. (2008) *Chem. Phys. Lipids* **154,** 64–67
42. Schlame, M. (2008) *J. Lipid Res.* **49,** 1607–1620
43. Mileykovskaya, E., and Dowhan, W. (2000) *J. Bacteriol.* **182,** 1172–1175
44. Mukhopadhyay, R., Huang, K. C., and Wingreen, N. S. (2008) *Biophys. J.* **95,** 1034–1049
45. Wang, X., Bogdanov, M., and Dowhan, W. (2002) *EMBO J.* **21,** 5673–5681
46. Mannock, D. A., Lewis, R. N., McElhaney, R. N., Harper, P. E., Turner, D. C., and Gruner, S. M. (2001) *Eur. Biophys. J.* **30,** 537–554
47. Osterberg, F., Rilfors, L., Wieslander, A., Lindblom, G., and Gruner, S. M. (1995) *Biochim. Biophys. Acta* **1257,** 18–24
48. Oradd, G., Andersson, A., Rilfors, L., Lindblom, G., Strandberg, E., and Andren, P. E. (2000) *Biochim. Biophys. Acta* **1468,** 329–344
49. Murzyn, K., Rog, T., and Pasenkiewicz-Gierula, M. (2005) *Biophys. J.* **88,** 1091–1103
50. Howard, K. P., and Prestegard, J. H. (1996) *J. Am. Chem. Soc.* **118,** 3345–3353
51. Jarrell, H. C., Jovall, P. A., Giziewicz, J. B., Turner, L. A., and Smith, I. C. (1987) *Biochemistry* **26,** 1805–1811
52. Andersson, A. S., Demel, R. A., Rilfors, L., and Lindblom, G. (1998) *Biochim. Biophys. Acta* **1369,** 94–102
53. Iwamoto, K., Sunamoto, J., Inoue, K., Endo, T., and Nojima, S. (1982) *Biochim. Biophys. Acta* **691,** 44–51
54. Thurmond, R. L., Niemi, A. R., Lindblom, G., Wieslander, A., and Rilfors, L. (1994) *Biochemistry* **33,** 13178–13188
55. van der Does, C., Swaving, J., van Klompenburg, W., and Driessen, A. J. (2000) *J. Biol. Chem.* **275,** 2472–2478
56. Sun, C., Rusch, S. L., Kim, J., and Kendall, D. A. (2007) *J. Bacteriol.* **189,** 1171–1175
57. Tsatskis, Y., Khambati, J., Dobson, M., Bogdanov, M., Dowhan, W., and Wood, J. M. (2005) *J. Biol. Chem.* **280,** 41387–41394
58. Guan, L., Smirnova, I. N., Verner, G., Nagamori, S., and Kaback, H. R. (2006) *Proc. Natl. Acad. Sci. U. S. A.* **103,** 1723–1726
59. Navarro, J., Toivio-Kinnucan, M., and Racker, E. (1984) *Biochemistry* **23,** 130–135
60. Goss, R., Lohr, M., Latowski, D., Grzyb, J., Vieler, A., Wilhelm, C., and Strzalka, K. (2005) *Biochemistry* **44,** 4028–4036
61. Qin, L., Hiser, C., Mulichak, A., Garavito, R. M., and Ferguson-Miller, S. (2006) *Proc. Natl. Acad. Sci. U. S. A.* **103,** 16117–16122
62. Katona, G., Andreasson, U., Landau, E. M., Andreasson, L. E., and Neutze, R. (2003) *J. Mol. Biol.* **331,** 681–692